2026 Volume: 02 Issue: 01 www.ijrpa.com ISSN 2456-9995 Research Article

International Journal Research Publication Analysis

Page: 01-13

MODELLING AND ANALYSIS OF THE CHARACTERISTICS OF THYRISTOR FIRING IN THE OPERATION OF CHOPPER DRIVE FOR DC MOTOR SPEED CONTROL

***Jonathan Amabikutol Emmanuel and Amasa Ukwuoma Emmanuel**

Department of Electrical and Electronic Engineering, Federal University Otuoke, Nigeria.

Article Received: 13 December 2025
Article Revised: 1 January 2026
Published on: 20 January 2026

***Corresponding Author: Jonathan Amabikutol Emmanuel**
Department of Electrical and Electronic Engineering, Federal University Otuoke, Nigeria.

DOI: https://doi-doi.org/101555/ijrpa.1668

ABSTRACTS:

Direct Current (DC) motors are used in industries because they are less expensive, offer reduced complexity in control structure, and provide wide speed and torque performance. The speed control was achieved for separately excited DC motor by varying the armature voltage and by varying field flux. speed control method by varying armature voltage using chopper. The firing circuit of chopper receives signal from controller and variable voltage is given to the armature of DC motor according to the desired speed. Different firing angles were considered. As the triggering angle increases, the load voltage and load current decrease. At a trigger angle of 0º, the load voltage and load current was 345.8V and 328.1A respectively and this highest magnitude of load voltage and load current. Furthermore, the simulation results showed that the highest speed was obtained when the trigger angle was 0º. This can be attributed to the fact that as the load current increases the speed of the DC motor rises. Therefore, since the lowest value of load voltage and load current were obtained at a trigger angle of 90º, the lowest speed of the DC motor was achieved in this case.

KEYWORDS: Direct current motor, Firing circuit, Chopper, Speed control, Load voltage and current

INTRODUCTION

For a long time, DC motors have been applied in variable speed drives. The extensive use of DC motors in industry can be attributed to their flexible control characteristics. High starting torques are provided by DC motors which is required for traction drives. Both low and high rated speed can be easily achieved, indicating control over large speed range. Compared to

Alternating Current (AC) motors, simpler and less expensive speed control methods can be realized with DC motors.

Usually, both series and Separately Excited DC Motors (SEDCM) are applied in variable speed drives. In traction applications, series motors are traditionally used. Presently, widely used motor drive systems in industry are the SEDCMs that are controlled by thyristor converters. With thyristor converter, variable armature voltage is provided for the drive motor. There are three basic methods to obtain a variable DC output voltage from a constant AC or DC supply voltage are: chopper control, integral cycle control, and phase control. The supply is connected to and disconnect from the motor terminals in all the methods by thyristor. The switching frequency is rapid. Thus, the average output voltage level is responded to by the motor and not to the individual voltage pulses.

Many researchers have studied DC motor control in literature. Speed response of performance of DC motor was improved using fractional order Proportional Integral and Derivative (PID) controller whose parameters were optimized by Genetic Algorithm (GA) and Integral Time Absolute Error (ITAE) compared to conventionally tuned PID method (Wati *et al.*, 2020). PID controller and fuzzy Logic Controller (FLC) were separately used to control the speed of DC motor, resulting in the later offering better performance (Kumar *et al*., 2014). The speed of DC motor was separately controlled with conventional PID, Internal Model Controller (IMC), and FLC (Ahmad *et al*., 2014). Technical review of position and speed control of Brushless DC (BLDC) motors with sensorless techniques and application trends revealed that most relevant were Sliding-mode observer, Extended Kalman Filter (EKF), Model Reference Adaptive System, Adaptive observers, and Artificial Neural Networks (ANN) (Gamazo-Real *et al*., 2010). The speed performance of chopper fed DC motor was enhanced using PI and PID controllers, respectively (Nandhini *et* al., 2017; Muoghalu *et al.*, 2021). The performance of DC motor was evaluated in terms of the relation between the speed and the load torque under different voltages (Popoola *et al*., 2015). Pulse Width Modulation (PWM) based speed control system for DC motor was implemented by Islam and Tripathi (2016) and Faroqi *et al*. (2018). The performances of IMC and PID in speed control system of DC motor was evaluated in MATLAB (Ahmed *et al*., 2020).

The studies by other authors as reviewed are all good and have helped in various ways in providing solution to DC motor speed control. Nevertheless, it could be observed from the reviews that they still have various limitations and vulnerabilities as some of

them could be either unstable, impossible to vary at low voltage, very expensive and have dead time of one second which gives the system low speed of response. It is on this note that this paper is designed to investigate and simulate DC Motor speed control by evaluating its performance under changing varying firing angle of the thyristor. This offers the advantage of durable and stable DC motor speed control with high speed of response without using complicated circuitry and costly components.

2. METHODOLOGY

2.1 Mathematical Modelling of DC Motor

Figure 1 shows the schematic circuit diagram of SEDCM. In the circuit, E_a is the terminal voltage applied to the motor, R_a and L_a are the resistance and inductance of the armature circuits respectively. R_f and L_f are the resistance and inductance of the field circuit respectively, E_b is generated back emf and T_m is the electromagnetic torque developed by the motor.

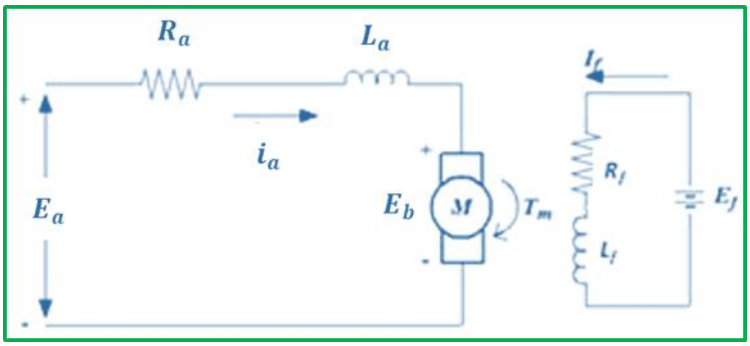

Figure 1: Schematic circuit of SEDCM.

As a result of the interaction between the field flux and the armature conductor, a torque is produced by the motor given by:

$$T_m = k_t \Phi i_a \quad (1)$$

where k_t is the motor torque constant, Φ field flux, and i_a is the armature current. The rotation of the armature and the flux linking its winding vary with time. Therefore, by Faraday's law, an Electromotive Force (EMF) is induced. This results in a back EMF given by:

$$E_b = k_t \Phi \quad (2)$$

Applying KVL in the armature circuit gives:

$$E_a = i_a R_a + L_a \frac{di_a}{dt} + E_b \quad (3)$$

In steady state condition, Equation (3) can be expressed as:

$$E_a = I_a R_a + E_b \quad (4)$$

In terms of torque and speed, the steady state equation will be given by Equation (5):

$$E_a = \frac{T_m}{k_t \Phi} R_a + k_t \omega \Phi \quad (5)$$

Such that the speed is given by:

$$\omega = \frac{E_a}{k_t \Phi} - \frac{T_m}{(k_t \Phi)^2} R_a \quad (6)$$

Thus, from the above equation it is clear that speed can be controlled by varying three parameters, namely, E_a, R_a, and Φ

3.2 Thyristor based Technique of DC Motor Speed Control

A single-phase full converter drive offers a two-quadrant drive operation and is limited to applications up to 15kW, which is shown in Figure 2. The armature converter gives $+V_o$ or $-V_o$ and allows operation in the first and fourth quadrant. The converter in the field circuit could be semi, full or even dual converter. The reversal of the armature or field voltage allows operation in the second and third quadrant.

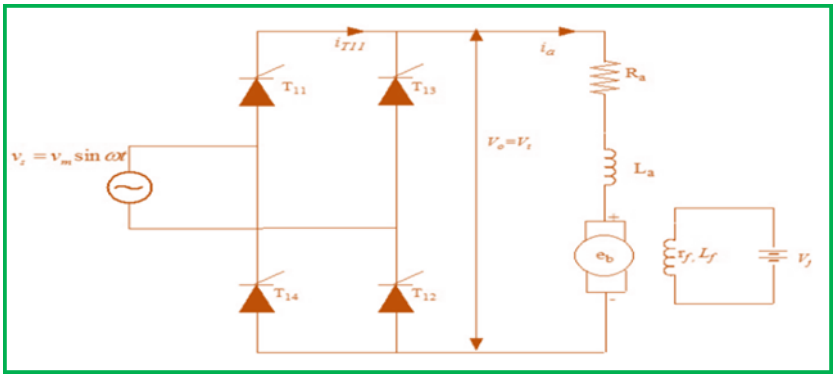

Figure 2: Single phase full wave converter drive.

The average armature voltage in armature circuit for single phase full converter drive is given by Equation (7):

$$V_o = V_t = \frac{2V_m}{\pi}(1 + \cos \alpha), \quad 0 < \alpha < \pi \quad (7)$$

In this work three phase fully, controlled rectifier fed separately excited DC motor is presented in this work.

2.3 Thyristor Three-phase Bridge Full-wave Controlled Rectifier Circuit

The thyristor three-phase bridge full-wave controlled rectifier circuit shown in Figure 3 is a typical form of AC/DC conversion. The function of this circuit is to convert three-phase AC power into DC power, with the average value of the output voltage changeable by use of a three-phase controllable rectifier bridge arm. The output value is controlled by the thyristor conduction angle. The output of the circuit relates to the load, which generally includes a pure resistor load, an inductive resistance load and back electromotive force load. The inductive resistance load is divided into high inductance and low inductance. So, there are four main circuit structures.

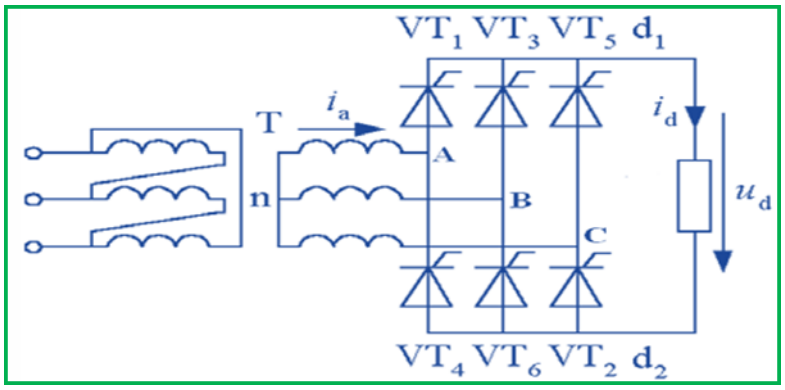

Figure 3: Thyristor three-phase bridge full-wave controlled rectifier circuit.

This work focuses on the analysis of the workings of the thyristor three-phase bridge full-wave rectifier circuit and also the speed and torque performance of separately excited DC motor (SEDCM). That the analysis includes: the voltage across the load, the current waveform, the trigger pulse sequence, and the speed and the torque.

2.4 Simulink Modelling

2.4.1 Simulink Model of Thyristor Three-phase Bridge Rectifier Circuit

Figure 4 is a simulation model of the thyristor three-phase bridge rectifier circuit. The Rectifier Bridge is the core unit of the thyristor three-phase bridge rectifier circuit, which is simulated using the Universal Bridge module in the MATLAB SimPowerSystems toolbox. This module has four input terminals and two output terminals.

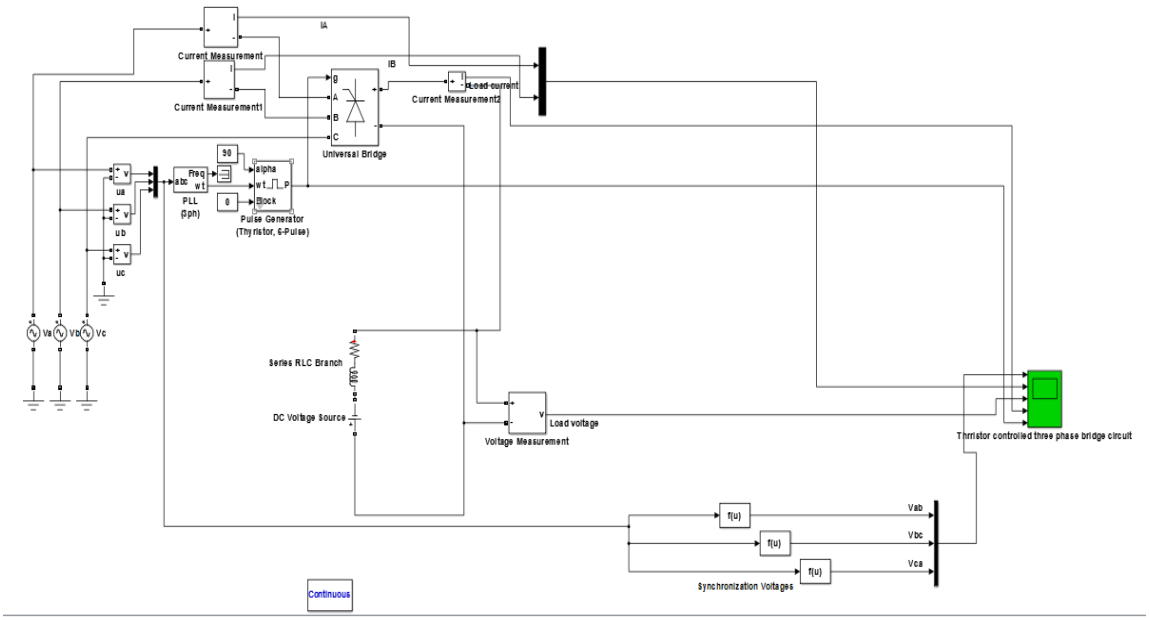

Figure 4: Simulation model of the thyristor three-phase bridge rectifier circuit.

wherein: A, B, C terminals are input terminals of the phase voltage of the three-phase AC power supply, and the g terminal is the trigger input terminal. +, - terminals: the output and input terminals of the rectifier circuit, which form a loop in the model.

The synchronised 6-pulse generator is used for triggering the six thyristors of the thyristor three-phase full-wave controlled bridge rectifier circuit. It has five inputs and one output terminal. Alpha_deg is the input terminal of the pulsed triggering angle control signal. Pulses are through the pulse output signal terminal, which is connected to the pulse input terminal of the three-phase bridge rectifier circuit. The pulse width is 10. The firing system of pulse generator mode is shown in Figure 5.

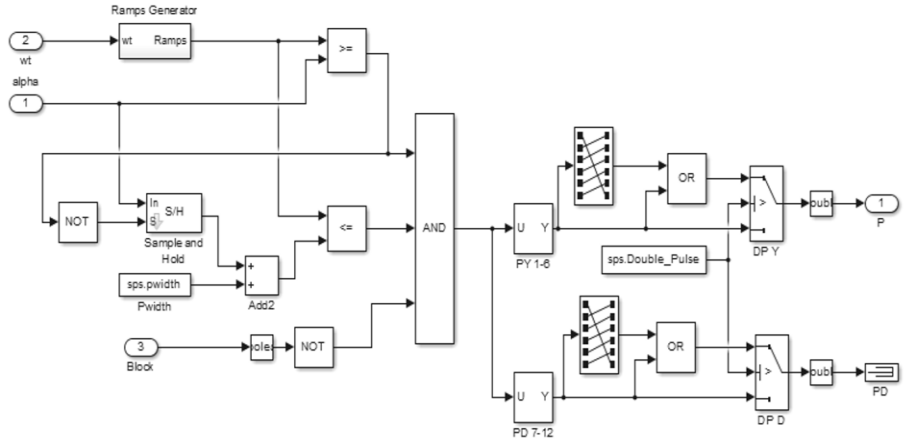

Figure 5: Pulse generator firing circuit.

The Phase Locked Loop (PLL) system can be used to synchronise on a set of variable frequency, three-phase sinusoidal signals. The frequency of synchronisation voltage is set to 50 Hz.

2.4.2 Simulink Model of Three-phase fully Control Rectifier Fed SEDCM

The developed Simulink model of the three-phase fully control rectifier fed separately excited DC motor (SEDCM) is shown in Figure 6. The Simulink model was used to get torque speed characteristic for a single-phase full converter drive. The effect of armature voltages on the torque speed characteristic is observed for five different firing angles, as the voltage applied to the field circuit is kept constant at 300 V, and a constant 200V (default value), 50 Hz AC is applied to input of single-phase full converter. The average value of applied armature voltage is varied by varying the firing angle of full converter.

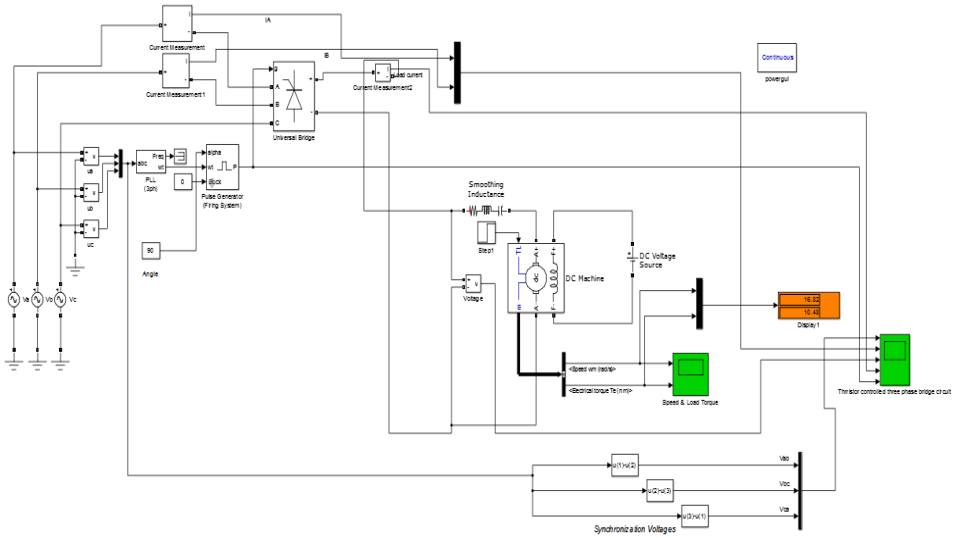

Figure 6: Simulink model of three-phase fully controlled rectifier fed SEDCM Motor.

2.5 Simulation Parameters

The values of the components used for the simulation in this work are given in Table 1.

Table 1: Simulation Parameters.

Components	Parameters
AC Voltage Source	Peak voltage = 200 V, Frequency = 50 Hz
PLL	Minimum frequency = 50 Hz, Initial inputs = [0 degree, 50 Hz], regulator (or controller gain) = [k_p, K_i, K_d] = [180, 3200, 1], Time constant = 0.003second,
Generator pulses (type 6-pulse)	Pulse width = 10
Load torque	10 Nm

DC motor	Horse power = 5 hp, supply voltage = 240 V, speed = 1750 rpm, Field voltage = 200 V
Universal Bridge (thyristor)	Snubber Resistance (R) = 1×10^5 Ω, Inductance = 1mH
RLC circuit	Resistance, R = 1 Ω, respectively, inductance = 1mH

RESULTS AND DISCUSSION

In this section, the results of the simulations conducted to evaluate the performance of the designed thyristor-based speed control technique of separately excited DC motor. Setting the value of the inductance L, resistance R and the value of the back electromotive force V, the four kinds of circuit are easily obtained. Also, setting the value of the alpha_deg parameter, the size of the phase shift control angle is easily set, and the output waveform of the rectifier circuit is obtained.

Figures 7 to 1 are the synchronized voltage of the supply, the waveform of iA and iB (current measurement of supply A and B), load voltage V_d, load current i_d and synchronised 6-pulse generator p when the trigger angle is 0º (Figure 7), 30º (Figure 8), 45º (Figure 9), 60º (Figure 10), and 90º (Figure 411), The load parameters are R = 1 Ω, L = 1 mH, back electromotive V = -5 V.

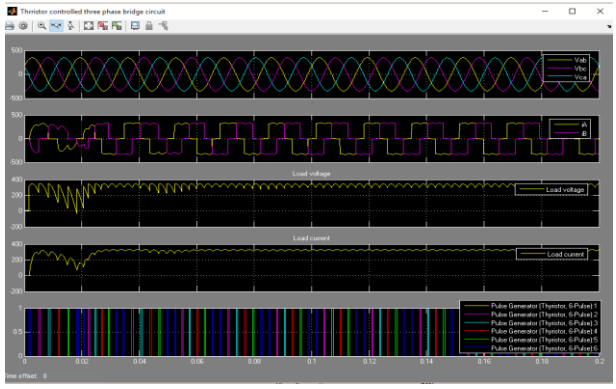

Figure 7: Waveform of the system output voltage and current. (trigger angle is 0º)

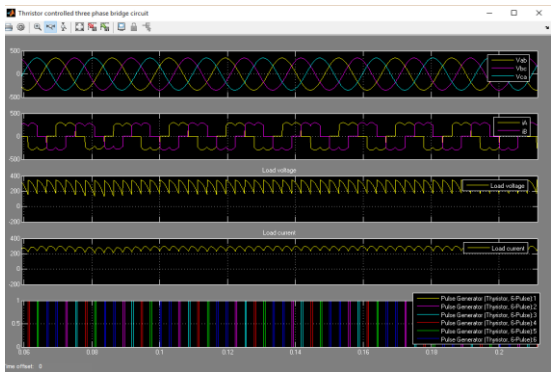

Figure 8: Waveform of the system output voltage and current. (trigger angle is 30º)

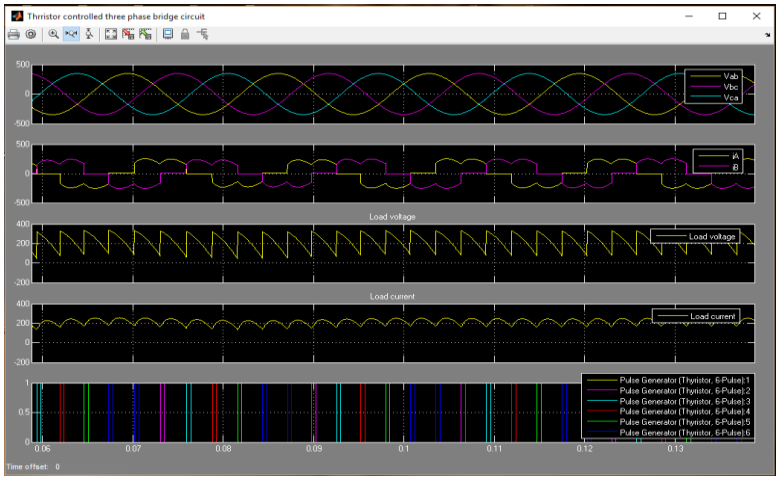

Figure 9 Waveform of the system output voltage and current (trigger angle is 45º)

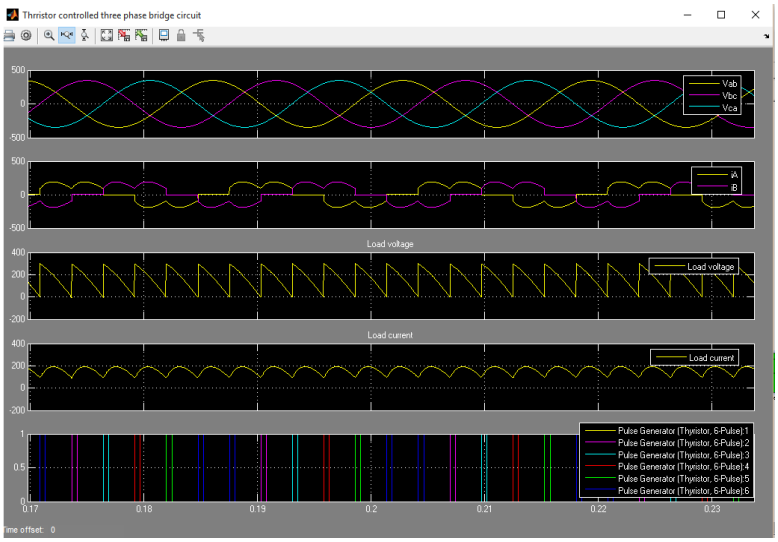

Figure 10: Waveform of the system output voltage and current (trigger angle is 60º)

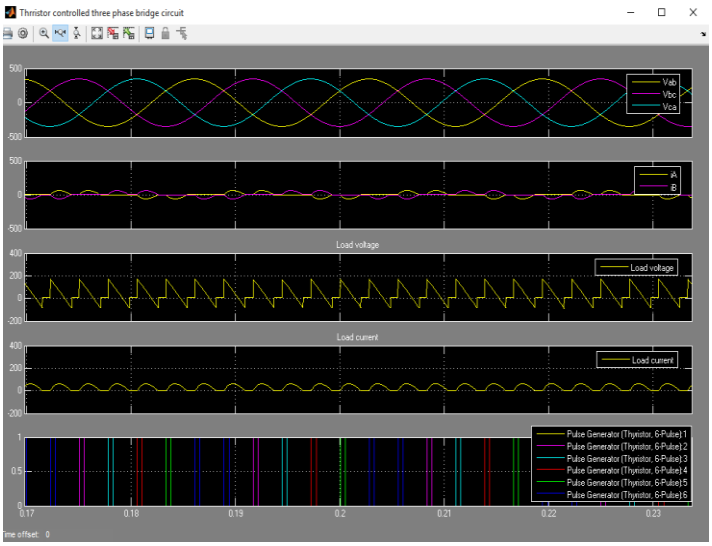

Figure 11: Waveform of the system output voltage and current (trigger angle is 90º)

It can be seen from Figures 7 through 11 that as the triggering angle increases, the load voltage and load current decrease. At a trigger angle of 0º, the load voltage and load current was 345.8V and 328.1A respectively and this highest magnitude of load voltage and load current. The results of the load voltage and current for the five triggering angles considered are shown in Table 2.

Table 2 Load voltage and load current performance.

Trigger Angle (º)	Load Voltage (V)	Load Current (A)
0º	345.8	328.1
30º	172.7	241.6
45º	172.8	227.5
60º	172.8	190.7
90º	5	7.5×10^{-5}

The resulting DC motor speed and load torque response with respect to the trigger angle is shown in Figures 12 to 16.

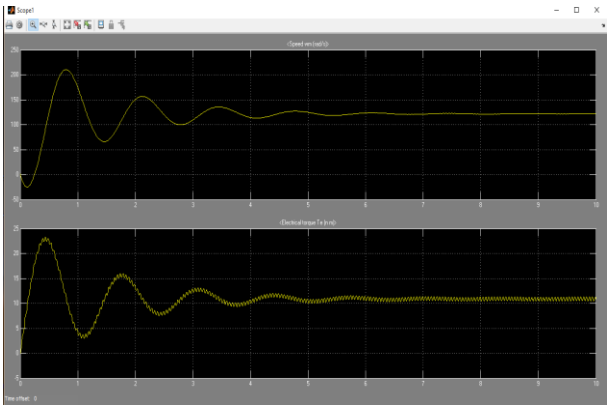

Figure 12: Speed and torque performance (trigger angle is 0º)

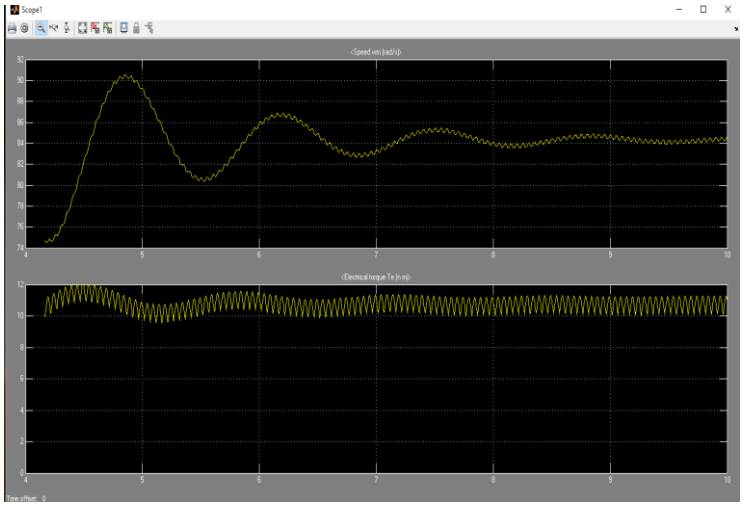

Figure 13: Speed and torque performance (trigger angle is 30º)

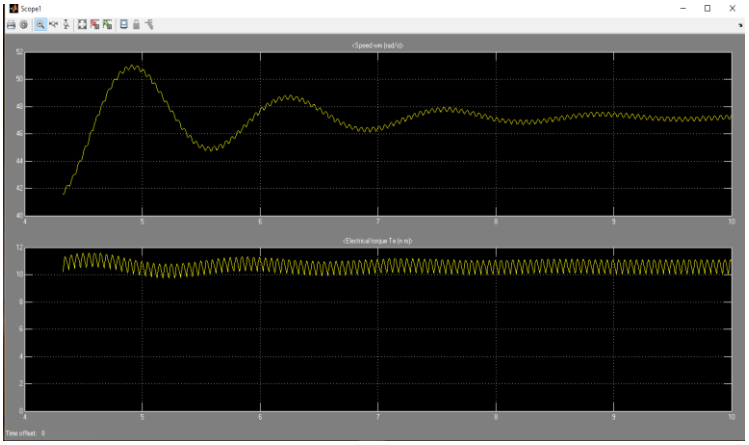

Figure 14: Speed and torque performance (trigger angle is 45º)

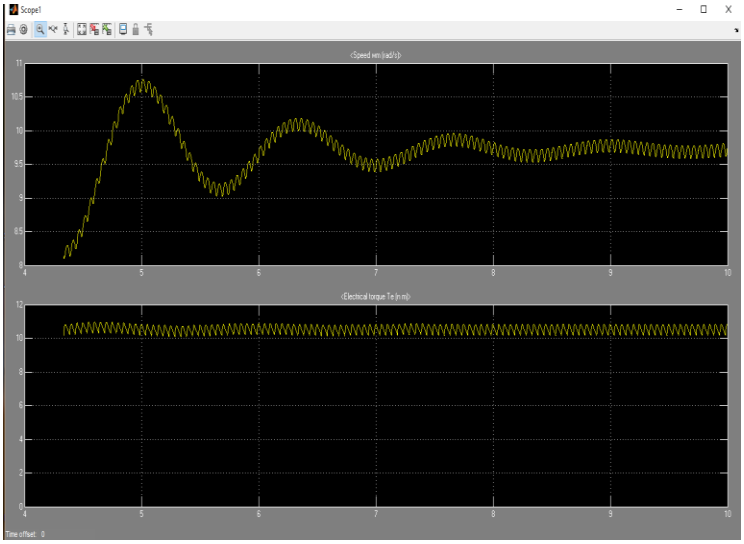

Figure 15: Speed and torque performance (trigger angle is 60º)

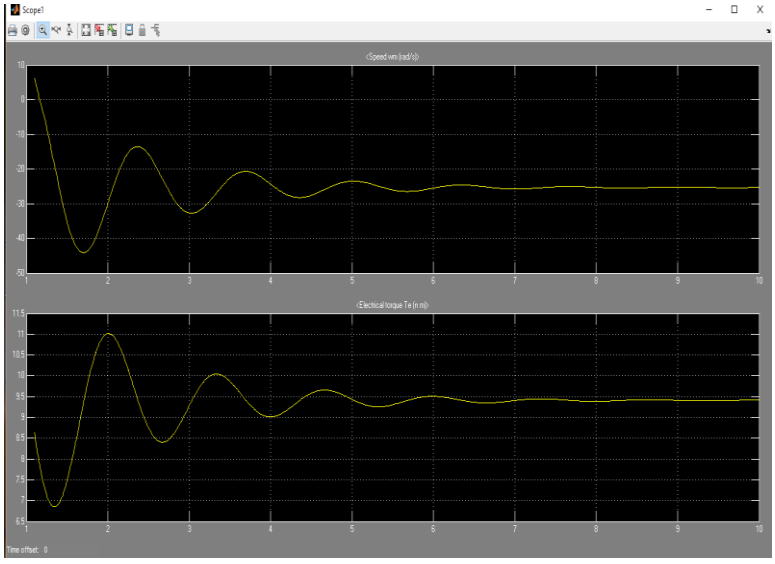

Figure 16: Speed and torque performance (trigger angle is 90º)

The simulation results showed that the highest speed was obtained when the trigger angle was 0º. This can be attributed to the fact that as the load current increases the speed of the DC motor rises. Therefore, since the lowest value of load voltage and load current were obtained at a trigger angle of 90º, the lowest speed of the DC motor was achieved in this case. Table 3 summarises the magnitude of the DC motor speed and toque with respect to the trigger angle.

Trigger Angle (º)	DC Motor Speed (rad/s)	Load Torque (Nm)
0º	122	10.88
30º	84.58	11.05
45º	47.33	11.01
60º	9.727	10.82
90º	-35.52	9.48

Generally, a thyristor-based speed control scheme of separately excited DC motor has been implemented. The speed was controlled using the three-phase full wave bridge rectified circuit fed excited DC motor. Simulation showed that as the firing angle increases the current decreases and this also causes the speed of the motor to drop.

CONCLUSION

This work has presented modelling and evaluation of the characteristics of firing circuit in the operation of chopper drive for DC Motor speed control. The analysis of the circuit shows that the motor speed for three-phase fully controlled rectifier fed DC motor was effectively regulated by varying the firing angle.

REFERENCES

1. Ahmed, U. O., Patrick, A. A., & Kwembe, B. A. (2020). DC motor speed control using internal model controller: industrial transformation strategy. *International Journal of Engineering and Advanced Technology, 9*(5), 300-306.
   DOI: 10.35940/ijeat.E9319.069520
2. Ahmad, Md A., Kishor, K., & Rai, P. (2014). Speed control of a DC motor using controllers. *Automation, Control and Intelligent Systems*, 2(6-1), 1-9.
   Doi: 10.11648/j.acis.s.2014020601.11
3. Faroqi, A., Ramdhani, M. A., Frasetyio, F., & Fadhil, A. (2018). DC motor speed controller design using pulse width modulation. *IOP Conf. Series: Materials Science and Engineering, 434*, 012205. doi:10.1088/1757-899X/434/1/01220

4. Gamazo-Real, J. C., Vázquez-Sánchez, E., & Gómez-Gil, J. (2010). Position and speed control of brushless DC motors using sensorless techniques and application trends. *Sensors*, *10*, 6901-6947. doi:10.3390/s100706901
5. Islam, M. S. & Tripathi, V. K. (2016). A study of D.C motor speed control through pulse width modulation implemented by MATLAB simulation. *International Journal of Advanced Research in Computer and Communication Engineering*, *5*(6), 219-223. DOI 10.17148/IJARCCE.2016.5647
6. Kumar, P., Kumar, P., Kumar, M., & Choudhary, S. D. (2014). Speed control of dc motor using PID & smart controller. *International Journal of Scientific & Engineering Research, 5*(11), 1044-1053.
7. Muoghalu, C. N., Ndefo, M. I., & Ugwu, H. I. (2021). Performance enhancement of chopper fed dc motor speed control system using PID controller. *Multidisciplinary International Journal of Research and Development, 1*(2), 1-8.
8. Nandhini, R., Kiruthika, J. K., Keerthana, G., Deepika, S., & Nagarajan, R. (2017). Chopper fed speed control of separatly excited DC motor using PI controller. *International Journal of Engineering Research & Technology*, *5*(13), 1-4.
9. Popoola, J. J., Oladejo, O. J., & Odeyemi, C. S. (2015). Modelling and simulation of armature controlled direct current motor using MATLAB. *SSRG International Journal of Electrical and Electronics Engineering*, *2*(3), 12-18.
10. Wati, T., Subiyanto, & Sutarno (2020). Simulation model of speed control DC motor using fractional order PID controller. *Journal of Physics: Conference Series, 1444*, 012022. doi:10.1088/1742-6596/1444/1/012022